# Lesions within and around the Pituitary

## Much More than Adenomas ...

Arnd Doerfler, Gregor Richter[1]

**Abstract**
The pituitary and parasellar region is an anatomically complex area where a number of neoplastic, infectious, inflammatory, developmental and vascular pathologies can occur. Differentiation among various etiologies may not always be easy, since many of these lesions may mimic the clinical, endocrinologic and radiologic presentations of pituitary adenomas. The diagnostics of sellar lesions involves a multidisciplinary effort, and detailed endocrinologic, ophthalmologic and neurologic testing is essential. CT and, mainly, MRI are the imaging modalities to study and characterize normal anatomy and the majority of pathologic processes in this region.
This article provides an overview of the relevant radiologic characteristics together with clinical findings of pituitary tumors, vascular, inflammatory and infectious lesions found in the pituitary and parasellar region in order to propose an appropriate differential diagnosis.

**Key Words:** Adenoma · Infection · MR imaging · Parasellar · Pituitary gland · Vascular · Tumor

**Clin Neuroradiol 2008;18:5–18**
DOI: 10.1007/s00062-008-8001-0

### Raumforderungen rund um die Hypophyse. Mehr als nur Adenome ...

**Zusammenfassung**
Die Differentialdiagnostik tumoröser, entzündlicher und vaskulärer Läsionen der Hypophyse und parasellären Region ist häufig schwierig, da viele dieser Läsionen Hypophysenadenome klinisch, endokrinologisch und radiologisch imitieren können. Die selläre und paraselläre Region ist zudem anatomisch komplex und stellt den Neuroradiologen vor eine besondere Herausforderung – ein kleinvolumiges Organ in anatomisch und teilweise auch funktionell sehr enger Nachbarschaft zu einer Vielzahl von Nachbarstrukturen muss mit hoher Orts- und Kontrastauflösung abgebildet werden, um die oft nur wenige Millimeter großen Läsionen zu erfassen. Anatomische Varianten ohne Krankheitswert können die Differentialdiagnose zudem erschweren. Ein multidisziplinärer Ansatz auch mit detaillierter endokrinologischer Testung ist daher entscheidend. Die Magnetresonanztomographie hat als sensitivste Methode in der Diagnostik intra- und parasellärer Läsionen alle anderen bildgebenden Verfahren verdrängt.
Diese Arbeit gibt einen Überblick über die radiologischen Charakteristika der häufigsten Läsionen in der und um die Hypophyse.

**Schlüsselwörter:** Adenom · Entzündung · Hypophyse · Magnetresonanztomographie · Parasellär · Vaskulär · Tumor

## Introduction

Radiologic imaging of the pituitary gland and the parasellar region is challenging since the pituitary gland is a very small-volume organ in close neighborhood to many eloquent structures. Furthermore, imaging necessitates high-contrast and topographic resolution not to miss the often very subtle pathologies. Additionally, anatomic variations can render differential diagnosis difficult.

[1] Department of Neuroradiology, University Hospital of Erlangen Medical School, University of Erlangen-Nuremberg, Erlangen, Germany.

Received: November 21, 2007; revision accepted: January 31, 2008

Magnetic resonance imaging (MRI) is the modality of choice to provide multiplanar high-contrast images of the pituitary gland and its adjacent structures.

Computed tomography (CT) is used only for supplementary purposes, i.e., to look for bony changes or to exclude or visualize calcifications. Located in the bony pituitary fossa, the pituitary gland may be morphologically and functionally divided into two parts, the anterior (adenohypophysis) and posterior (neurohypophysis) lobe. Embryologically, the distal part of the adenohypophysis arises from the epithelium of Rathke's pouch, an invagination of the roof of the oropharyngeal membrane. As part of the brain, the neurohypophysis is composed of the neural stalk (infundibulum) and the neural lobe (infundibular process). The pars intermedia, derived from the posterior wall of Rathke's pouch, is located in between the anterior and posterior lobe and is usually not seen on MRI. The posterior lobe of the pituitary gland and the pituitary stalk receive their blood supply from the superior and inferior hypophyseal branch of the internal carotid artery, whereas the anterior lobe receives its blood supply from penetrating capillary loops from the portal vessels of the hypophyseal-portal circulation, respectively.

The adenohypophysis produces a variety of hormones, i.e., prolactin, growth hormone (GH), thyroid-stimulating hormone (TSH), follicle-stimulating hormone (FSH), and luteinizing hormone (LH). In addition, prohormone precursors of corticotropin (ACTH), and melanocyte-stimulating hormone are secreted, respectively. Thus, lesions of the adenohypophysis may cause hormone deficiency resulting in a variety of clinical symptoms.

The posterior pituitary lobe has no independent secretory function and receives vasopressin (ADH) and oxytocin from the hypothalamic neurons through the capillaries for storage. In newborns, up to 3 months of age, both anterior and posterior pituitary lobes exhibit hyperintensity on T1-weighted imaging [1, 2]. With increasing age, the adenohypophysis seems to lose its hyperintensity gradually, whereas the neurohypophysis remains hyperintense [3].

Experimental studies have shown, that the high signal intensity of the posterior lobe is caused by accumulated neurosecretory granules containing ADH (and not fat, as hypothesized before). Thus, in patients with a central diabetes insipidus, the high signal of the posterior lobe is absent, returning after appropriate medical substitution [4].

A standard protocol for MRI of the pituitary and parasellar region consists of thin-section (2–3 mm) sagittal and coronal T1-weighted images with and without contrast enhancement (Table 1, Figure 1). Angulation of the coronal images can vary, being either perpendicular to the sella turcica or parallel to the pituitary stalk. Thin-sectional T2-weighted imaging can be added to look for cystic lesions. Searching for pituitary pathologies, we administer half the standard dose of Gd-DTPA (0.05 mmol/kg). Additionally, one scan covering the whole brain (T2 or FLAIR) should be supplemented.

**Table 1.** MRI standard protocol.

- T1-weighted imaging, coronal, 3 mm
- T1-weighted imaging, sagittal, 3 mm
- T1-weighted imaging, coronal, 3 mm, enhanced
- T1-weighted imaging, sagittal, 3 mm, enhanced
- T2-weighted imaging, coronal, 3 mm, native

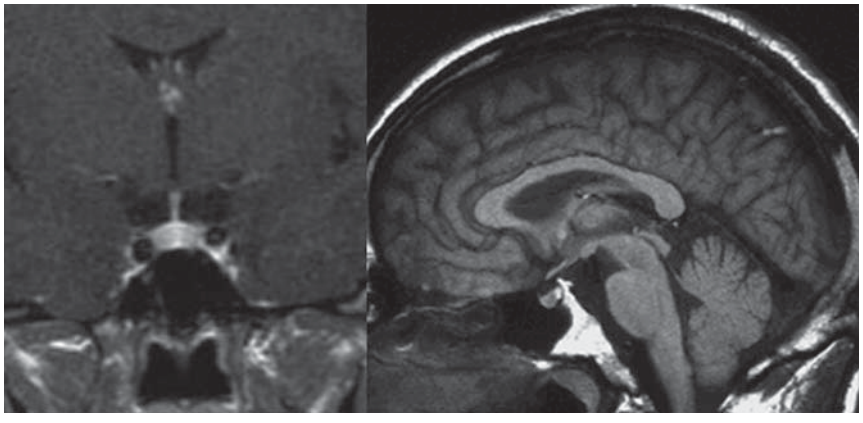

**Figure 1.** Normal pituitary gland (T1-weighted coronal und sagittal scans after contrast administration).

CT may become important when supplementary information concerning bony structures or calcifications is required. CT is frequently used in extensively growing pituitary adenomas, invading the sphenoid sinus, nasal cavity or the skull base. Additionally, anatomy of the sphenoid sinus can be evaluated prior to transsphenoidal surgery. To exclude acute pituitary hemorrhage, CT still may be helpful in the emergency situation.

Nowadays, conventional radiography is mainly obsolete in the diag-

nostic work-up of pituitary adenomas. Adenomas are usually very slow-growing lesions, resulting in a vertical and horizontal enlargement of the bony pituitary fossa (balloon sella) on plain film with no demineralization. Asymmetric growth of pituitary adenomas may lead to a double outline of the sellar floor in the lateral view. Thinning, destruction or dorsal shift of the dorsum sellae may also occur. Digital subtraction angiography is also not part of the routine work-up of pituitary and parasellar lesion, but still may be necessary to assess the parasellar vessels or exclude vascular pathology. However, with continuous improvement of noninvasive imaging modalities such as MR angiography (MRA) and CT angiography (CTA), conventional angiography is indicated only in very selective cases. In patients with central Cushing's disease with no adenoma visible on MRI, selective inferior petrous sinus venous blood sampling is a highly specific technique that might be helpful in the diagnosis and especially lateralization of the microadenoma and might guide the selective surgical resection.

## Congenital Lesions of the Sellar Region

### Rathke's Cleft Cyst

Most sellar epithelial cysts are remnants of derivates of Rathke's cleft and arise in the region of the pars intermedia. They are relatively common incidental findings at autopsy (up to 30%) usually remaining asymptomatic [5]. Location is usually intrasellar, between the anterior and posterior pituitary lobe (Figure 2), frequently configurated like a "baseball". Occasionally, they can occur in the suprasellar region, anterior to the infundibulum. Symptoms may result from mass effect leading to headache, endocrine dysfunction or visual impairment, due to compression of the optic chiasm. Differentiation from craniopharyngiomas is of particular importance but often difficult. Histologically, these lesions can be distinguished by the composition of their walls. Rathke's cleft cysts can contain mucinous or serous fluid and thus display variable density on CT and signal intensity on MRI. Cysts containing serous fluid are typically hypointense, whereas mucoid cysts show hyperintensity on T1-weighted images [5, 6]. Sometimes, differentiation from acute hemorrhage can be difficult. Clinical symptoms and follow-up imaging are of great importance in this setting.

### Arachnoid Cysts

While suprasellar arachnoid cysts usually present with symptoms due to the local mass effect in children, the rarer intrasellar arachnoid cysts are regarded as acquired and may become symptomatic later in life [7–9]. Clinical symptoms may include increased intracranial pressure, hormone deficiency, gait disturbance, and visual impairment. It is thought that arachnoid cysts arise from herniation of an arachnoid diverticulum through an incomplete diaphragma sellae. Although usually indistinguishable from Rathke's cleft cysts, they typically displace the anterior lobe and the infundibulum posteriorly [8]. On MRI, a focal mass with cerebrospinal fluid (CSF) signal intensity might be seen (Figure 3).

Volume reduction of the pituitary gland is commonly seen after pituitary apoplexy, radiotherapy or in the postpartum period. Whereas the pituitary gland often appears displaced toward the posterior inferior aspect of the pituitary fossa, the infundibulum remains in its normal midline position. Pseudotumor cerebri, also known as benign intracranial hypertension, is a condition marked by elevated CSF pressure [10, 11]. Almost 50% of patients with this condition are found to have a so-called empty sella, characterized by an intrasellar extension of the suprasellar cistern and a flattened pituitary gland [12].

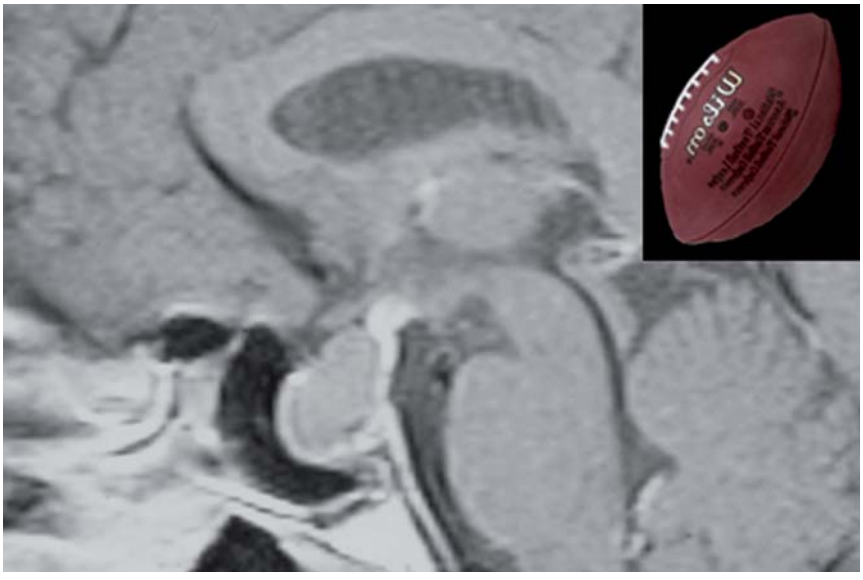

**Figure 2.** Rathke's cleft cyst (T1-weighted sagittal scan after contrast administration).

By contrast, pituitary hyperplasia might be a physiological response occurring at birth, puberty, pregnancy, and post partum [13, 14]. During puberty, the pituitary gland may reach 8–10 mm in height. During pregnancy, it can enlarge up to 10 mm in height and immediately post partum it may even measure 12 mm in height, respectively.

### Ectopic Posterior Lobe

An ectopic posterior lobe is usually not an incidental finding but is found in diagnostic imaging studies for GH deficiency [15–18]. It is thought to be a developmental anomaly, rather than caused by traumatic (birth) incidents. Patients become conspicuous with dwarfism and an isolated GH deficiency or multiple anterior pituitary lobe hormone deficiencies. On T1-weighted images, the ectopic posterior lobe is typically seen as a small nodule with characteristic high signal at the median eminence in the floor of the third ventricle [19–21] (Figure 4). Sometimes, a tender pituitary stalk can only be seen after contrast enhancement.

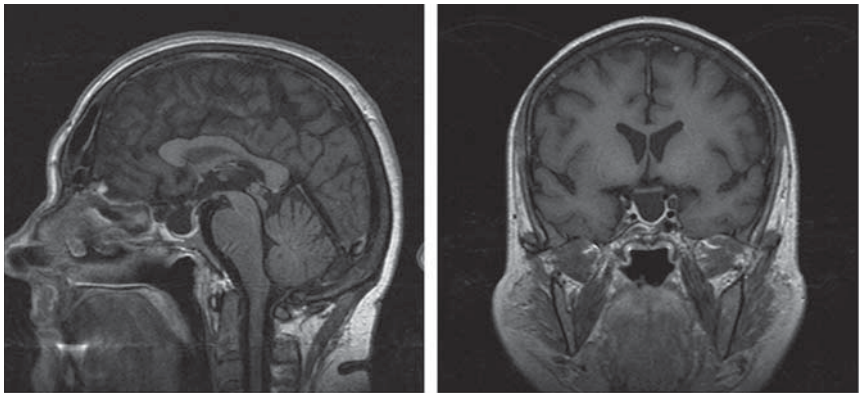

**Figure 3.** Intrasellar arachnoid cyst resulting in an „empty sella" (coronal and sagittal T1-weighted imaging after contrast administration).

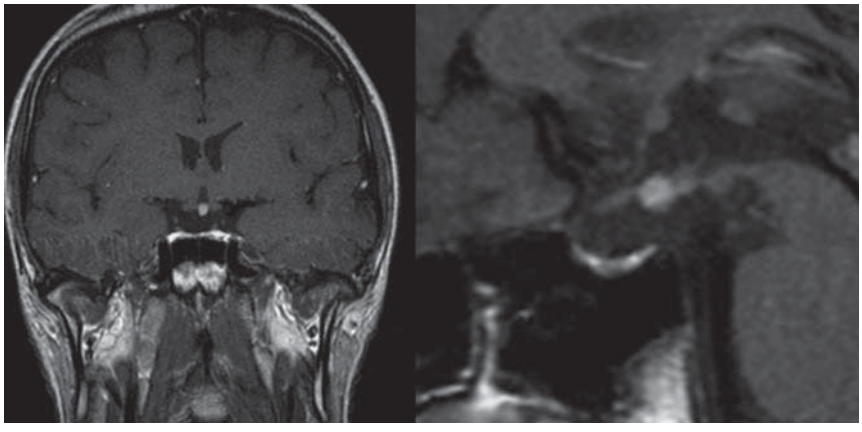

**Figure 4.** Ectopic posterior lobe on T1-weighted images (coronal and sagittal scans).

### Pituitary Adenomas

Pituitary adenomas are benign epithelial lesions and account for about 10–15% of all intracranial tumors representing the most common intrasellar pathology. In unselected autopsy series, the estimated incidence is found to be up to 27%. Using the size as a criterion, adenomas ≥ 10 mm are classified as macroadenomas, whereas lesions < 10 mm are referred to as microadenomas. Classification concerning endocrine function distinguishes hormone-secreting from nonsecreting (nonfunctional) tumors.

Prolactin secreting adenomas are the most common secretive tumors and account for about 30% of all pituitary adenomas. Clinical manifestations in women are secondary amenorrhea, galactorrhea, and infertility [22]. In men, loss of libido and impotence can occur [23, 24]. Because of their insidious symptoms, prolactinomas in men are often diagnosed at a later stage, when they are large enough to cause visual symptoms. Acromegaly in adults or gigantism in children are the cardinal symptoms of GH-producing adenomas [25]. Peak incidence is in the 5th life decade. Acromegaly is characterized by growth of feet and hands as well as coarsening of facial features. Retrospective studies indicate that mortality in acromegalic patients is approximately doubled relative to the general population, mostly due to cardiovascular events [26, 27]. Their insidious onset of the disease often leads to a significant delay in diagnosis. About 5–10% of pituitary adenomas cause elevated glucocorticoid levels (ACTH-producing adenomas). Overproduction leads to the stigmata of Cushing's disease, including diabetes, hypertension, osteoporosis, easy skin bruisability and striae, truncal obesity, moon facies, amenorrhea, impotence, and a generalized weakness. In children, growth retardation is a common manifestation [28]. Treat-

ment can either be surgically or with neuromodulatory drugs [29]. Patients with Cushing's disease, who cannot be controlled by pituitary surgery, may have to undergo bilateral adrenalectomy. Due to the abolition of negative feedback on the pituitary, ACTH-producing adenomas continue to grow even more after adrenalectomy (so-called Nelson's tumor) in about 15% [30, 31].

TSH-producing adenomas occur in < 1%, leading to hyperthyroidism [32]. Aberrant secretion of FSH and LH is very rare, causing symptoms such as hypogonadism. About 10% of all adenomas are mixed tumors, out of which 75% are macroadenomas. Nonfunctioning adenomas are the second most common tumors, accounting for 25–30% of pituitary adenomas. The majority of nonsecreting adenomas are macroadenomas and often grow to a significant size, causing visual field defects, hydrocephalus, or other mass effects. Parasellar infiltration into the cavernous sinus occurs in 40%, but rarely leads to cranial nerve palsies [33, 34]. Cranial nerve palsy in combination with a sellar mass should rather arouse suspicion of metastasis or ophthalmoplegic aneurysm [35, 36].

*Macroadenomas* are best evaluated with MRI. Since these tumors usually extend beyond the confines of the sella, infiltration of the cavernous sinus, the sphenoid sinus or the clivus, compression of the optic chiasm, and encasement of the internal carotid artery can be present [37]. Cavernous sinus invasion often restricts complete surgical tumor resection. In contrast to parasellar meningiomas, encasement of the internal carotid artery rarely causes luminal compromise in pituitary adenomas. In about 94% macroadenomas lead to enlargement of the bony pituitary fossa (Figure 5). Intratumoral hemorrhage of macroadenomas (Figure 6) occurs in up to 10–15% of incidental pituitary adenomas [38]. Medical treatment with bromocriptine as well as pregnancy are typical predisposing factors associated with apoplexy and pituitary hemorrhage [39, 40]. Primary pituitary hemorrhage may also occur posttraumatically, after surgery, after viral diseases or radiation therapy, or during delivery. Acute hemorrhagic infarc-

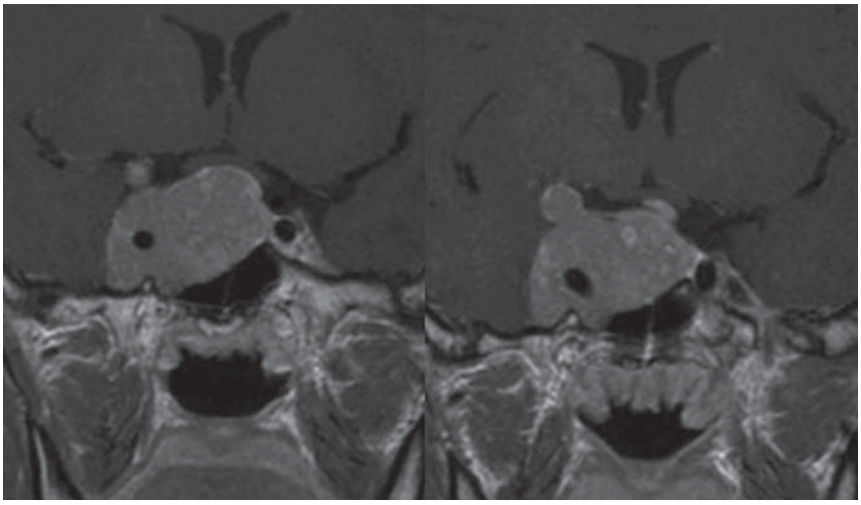

**Figure 5.** Macroadenoma of the pituitary gland with infiltration of the cavernous sinus, encasement of the internal carotid artery, and slight compression of the optic chiasm (T1-weighted coronal scans after contrast administration).

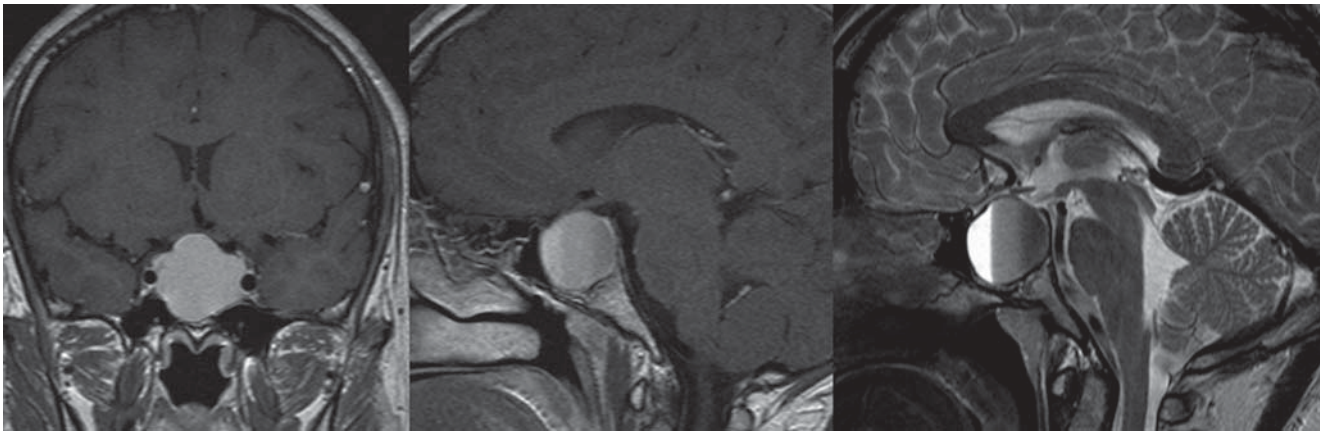

**Figure 6.** Acute hemorrhage of a pituitary macroadenoma, with enlargement of the bony pituitary fossa and compression of the optic chiasm (T1-weighted coronal und sagittal scans after contrast administration and T2-weighted sagittal imaging).

tion of a pituitary adenoma is referred to as pituitary apoplexy with an impressive clinical presentation, i.e., acute onset of headache, vomiting, ophthalmoplegia and visual loss [41, 42]. Rarely, meningism, depression of consciousness or seizures can occur.

*Microadenomas* are best seen on coronal images and usually appear hypo- or isointense relative to normal pituitary tissue on unenhanced T1-weighted images (Figure 7) [3, 43]. After contrast administration, due to an earlier and more intense enhancement of normal pituitary tissue, the microadenoma usually remains hypointense. Indirect radiologic features of microadenomas may be a one-sided elevation of the diaphragm or lateral sloping of the pituitary fossa. In dynamic sequences after rapid injection of contrast medium, a delayed enhancement of the adenoma may be seen [44–47]. Studies of normal pituitary tissue have also shown an earlier enhancement of the posterior lobe, due to the direct blood supply of the neurohypophysis via hypophyseal branches of the internal carotid artery. Using fast T1-weighted images, some microadenomas demonstrate an early arterial enhancement, occurring simultaneously as enhancement of the posterior lobe [48]. However, compared with normal pituitary tissue most microadenomas display a slightly lower signal intensity.

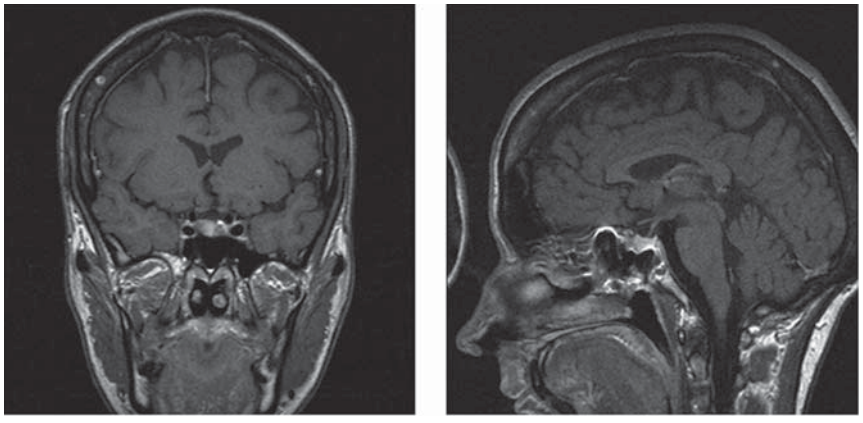

**Figure 7.** Microadenoma of the pituitary gland (T1-weighted coronal und sagittal scans after contrast administration).

### Postoperative Imaging

Postoperative imaging is essential, if residual tumor is suspected after incomplete resection of invasive pituitary adenomas. Also in case of persisting or recurring hormone disturbances, MRI is the modality of choice to visualize residual tumor (Figure 8). In nonfunctional pituitary adenomas, postoperative imaging remains the only method to prove complete resection. Comparison with preoperative scans and operative reports are of great importance in this setting. Postoperative studies have shown that the maximal extension of the pituitary mass does not return to normal immediately after surgery (even with total tumor removal). A baseline examination is therefore recommended 3 months after surgery. In the meantime, postoperative changes usually have resolved and the delay is not too long to risk significant growth from residual tumor [49]. Further control scans after 1 year have been proven useful. Studies have shown that contrast-enhanced imaging immediately (1st postoperative day) following resection may also be reliable to visualize residual tumor [50]. Fat-suppressed sequences enable discrimination between fat-packing or -enhancing adenoma.

## Other Pituitary Lesions

Primary tumors of the posterior lobe of the pituitary, e.g., pituicytomas or

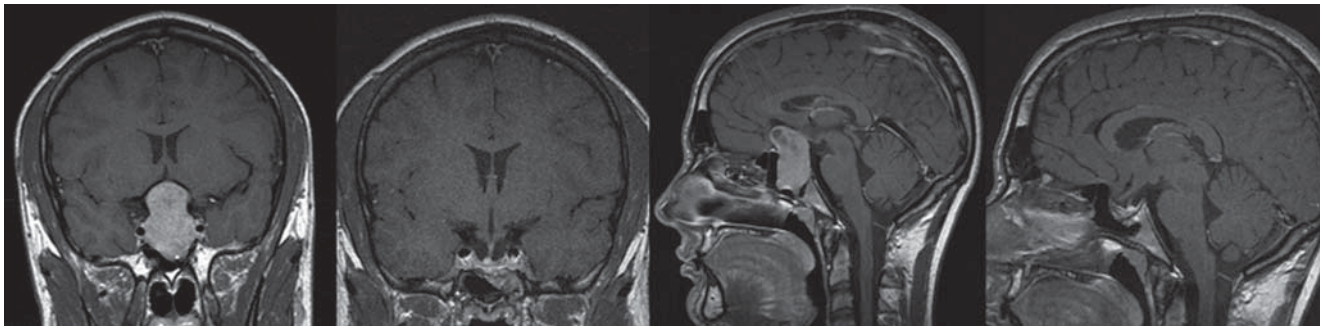

**Figure 8.** Macroadenoma of the pituitary gland with compression of the optic chiasm. Postoperative follow-up 3 months after surgery confirming complete surgical resection (T1-weighted coronal und sagittal scans after contrast administration).

gangliogliomas, are very rare lesions. Pituitary metastases most commonly arise from the common primaries such as breast, thyroid or lung cancer and occur in approximately 3% of terminally ill patients [51]. Interestingly, only about 5–15% of these patients become symptomatic [36]. Metastases tend to arise within the posterior lobe of the pituitary or the pituitary stalk and spread to the anterior lobe of the pituitary later. Typical MRI findings include a relatively small enhancing pituitary lesion and a lack of sella enlargement. Bony destruction may occur. Third nerve palsy in combination with a sellar mass rather points toward metastasis or ophthalmoplegic aneurysm. Rarely, pituitary adenomas can transform to pituitary carcinomas (0.1–0.5% of all pituitary tumors) [52, 53]. They are locally destructive and can metastasize to intracranial and intraspinal sites via CSF pathways. Hepatic, bronchial, osseous and lymphatic spread are also reported.

### Meningiomas

Meningiomas of the sellar region (cavernous sinus, planum sphenoidale, diaphragma sellae, clinoid process) account for 20–30% of all intracranial meningiomas. They are benign slow-growing tumors that can reach considerable size at the time of diagnosis. To distinguish meningiomas from neurinomas, dynamic contrast-enhancing MRI sequences are useful, since meningiomas usually show early enhancement, while neurinomas present gradual enhancement [54, 55]. Due to an en plaque growth pattern often associated with a "dural tail", differentiation from pituitary macroadenomas usually is not a problem (Figure 9). Pure intrasellar meningiomas are very rare and may be hard to distinguish from adenomas [56, 57]. They usually originate from the dorsum sellae. When invading into the cavernous sinus, meningiomas tend to constrict the carotid lumen, which is usually not a feature of adenomas [37, 58–60]. They often may cause hyperostosis at the sites of bony attachment.

### Craniopharyngiomas

Craniopharyngioma is an important differential diagnosis accounting for approximately 3% of all intracranial tumors. Usually slow-growing, craniopharyngiomas arise from squamous epithelial cell rests of Rathke's

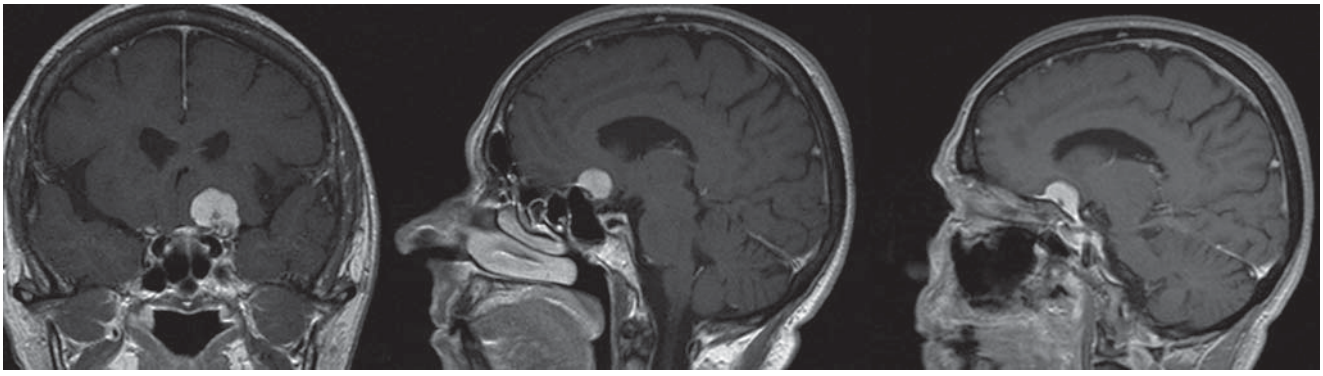

**Figure 9.** Left parasagittal meningioma of the planum sphenoidale with "dural tail" (T1-weighted coronal und sagittal scans after contrast administration).

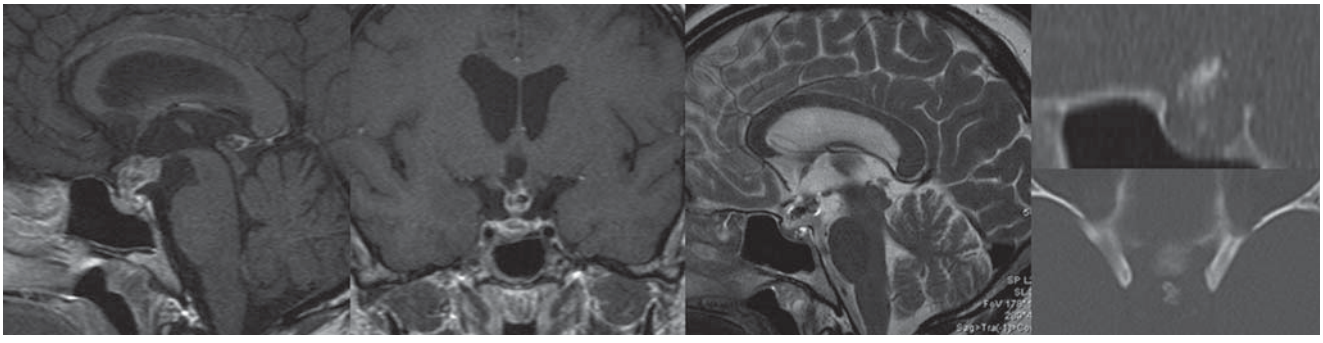

**Figure 10.** Suprasellar craniopharyngioma with cystic und solid components and typical suprasellar calcification in CT (contrast-enhanced sagittal and coronal T1-weighted imaging, T2-weighted sagittal imaging, and sagittal and axial plain CT).

pouch [61]. Craniopharyngiomas may be divided into adamantinomatous or squamous-papillary histological types [62]. In children, they make up about 5–10% of all intracranial neoplasms, being third in frequency to medulloblastoma and astrocytoma. Patients usually present with headache, visual impairment, hydrocephalus, or hypopituitarism. Although suprasellar in origin, about 50% of craniopharyngiomas extend into the sella. The suprasellar component of the craniopharyngioma may induce edema to spread along the optic tract [63, 64]. In CT and MRI, craniopharyngioma has a typical heterogeneous appearance with cystic and solid components and frequently (approximately 93%) abundant calcifications (Figure 10) [62, 65]. The solid tumor portions as well as the cyst wall enhance usually after contrast administration.

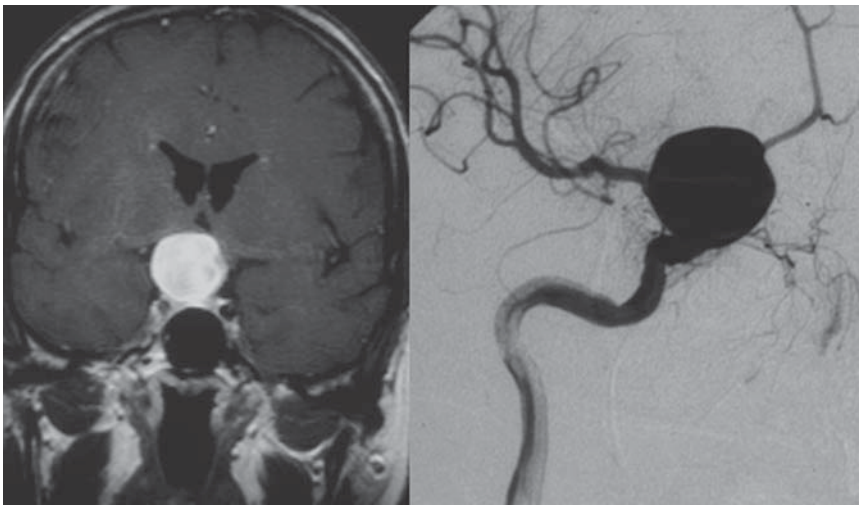

**Figure 11.** Paraophthalmic "giant aneurysm" of the right internal carotid artery with extension up to the optic chiasm (T1-weighted coronal scan after contrast administration and digital subtraction angiogram of the right internal carotid artery).

### Germ Cell Tumors

Intracranial germinomas occur most frequently in the pineal and suprasellar region but can also be primarily intrasellar [66, 67]. Occasionally, these tumors can extend to involve the sella turcica and simulate a pituitary macroadenoma. Germinomas usually show prominent contrast enhancement and present well-defined margins. Individual case reports describe sellar lesions that radiologically cannot be differentiated from pituitary adenomas, such as chondrosarcomas, granular cell tumors

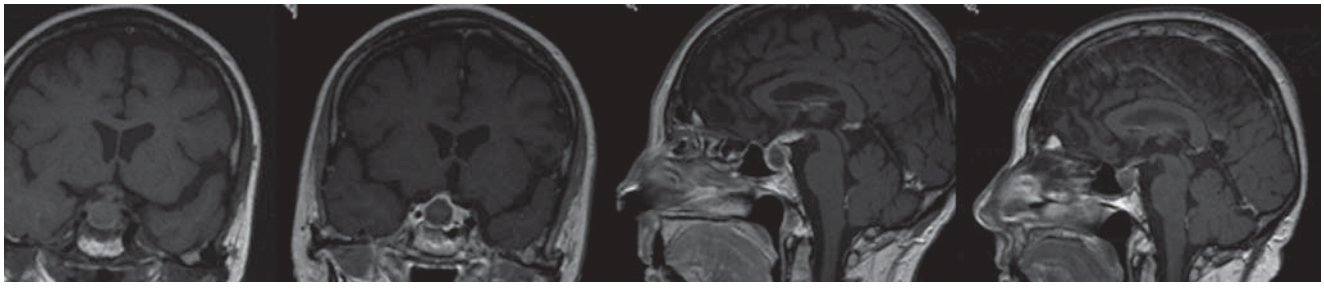

**Figure 12.** Hypophysitis with thickening of the pituitary stalk in combination with an intense contrast enhancement (coronal [before and after contrast administration] and sagittal T1-weighted imaging).

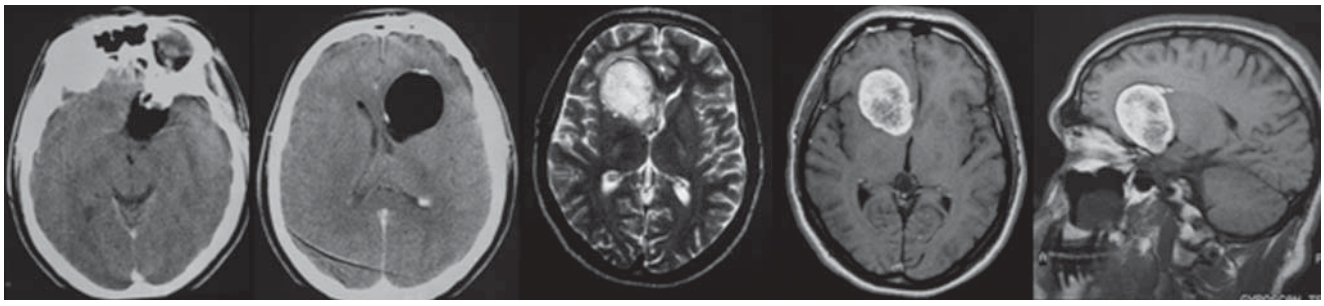

**Figure 13.** Para- and suprasellar dermoid (plain CT, axial T2-weighted and axial and sagittal T1-weighted imaging).

[68, 69], gangliocytomas [70, 71], fibrosarcomas [72, 73], hemangiopericytomas [74], esthesioneuroblastomas [75], melanomas [76], ependymomas [77], or lymphomas [78].

### Aneurysms

Aneurysms of the sellar region usually originate from the cavernous or supraclinoid portions of the internal carotid artery and account for up to 10% of all cerebral aneurysms. In selected cases, they can mimic other supra-, para- or intrasellar lesions [79]. MRI or CT are useful in differentiating tumor from thrombosed and nonthrombosed aneurysms (Figure 11). Usually, the aneurysm itself can be sufficiently visualized by noninvasive imaging using MRA or CTA.

### Inflammatory and Infectious Lesions

Sarcoidosis, a systemic disease featuring multiple noncaseating granulomas, may involve the central nervous system in about 5% of cases. Predilection sites are the leptomeninges, especially the sellar and suprasellar region, such as the pituitary stalk, optic chiasm and the hypothalamus, respectively [80]. Since radiologic differentiation from other diseases such as lymphocytic hypophysitis is often impossible, clinical history and time course are of great importance. Lymphocytic hypophysitis is a rare autoimmune inflammatory disease most often seen in women in the peri- or postpartum period. Clinical symptoms usually include diabetes insipidus, amenorrhea, hypopituitarism, headache, and visual impairment favorably responding to steroid therapy [81–83]. MRI usually demonstrates thickening of the pituitary stalk in combination with an intense contrast enhancement [84] (Figure 12). Granulomatous hypophysitis can occur with fungal infections, tuberculosis [85], sarcoidosis [86], Langerhans' cell histiocytosis, and Wegener's granulomatosis [87] and accounts for approximately 1% of sellar masses. The typical radiologic appearance is similar to that of lymphocytic hypophysitis [88, 89]. Pituitary abscess can be primary or secondary due to an adenoma or to surgical procedure [90]. Spread of gram-positive bacteria from the sphenoid sinus is another source of infection, but rare infectious diseases such as toxoplasmosis [91] or cryptococcosis have been described. Typical MRI findings are those of a round sellar mass with ring

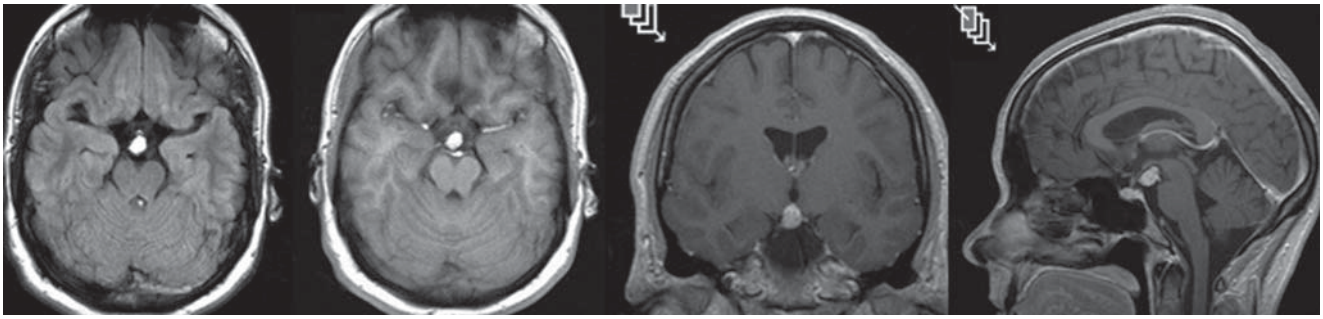

**Figure 14.** Suprasellar lipoma (axial FLAIR, T1-weighted axial [unenhanced], coronal and sagittal scans after contrast administration).

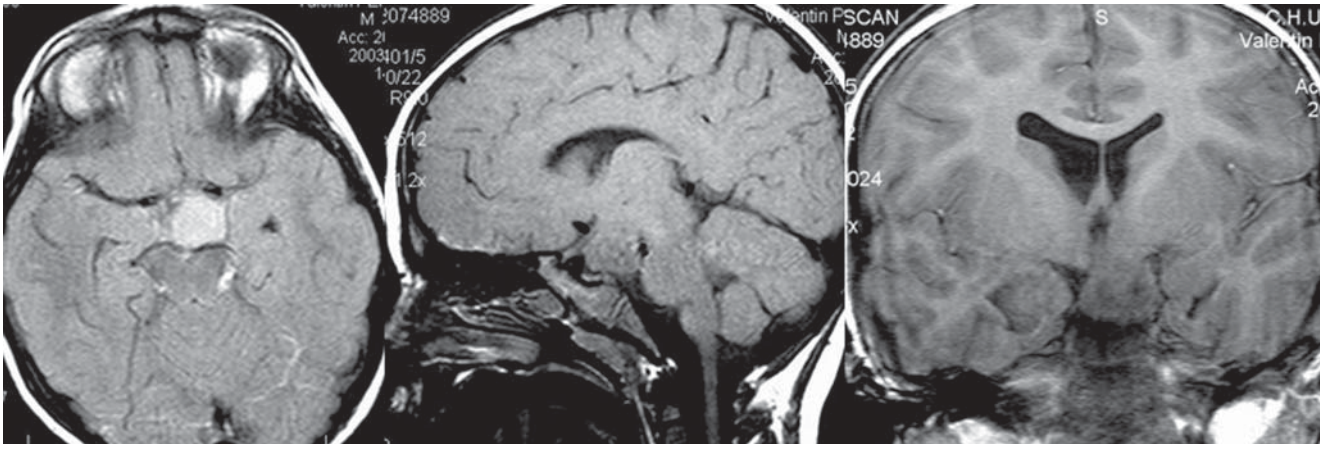

**Figure 15.** Hamartoma of the tuber cinereum (axial and sagittal FLAIR and coronal unenhanced T1-weighted imaging).

enhancement. Furthermore, meningeal enhancement due to concurrent meningitis may help distinguishing pituitary abscess from pituitary adenoma [92–94].

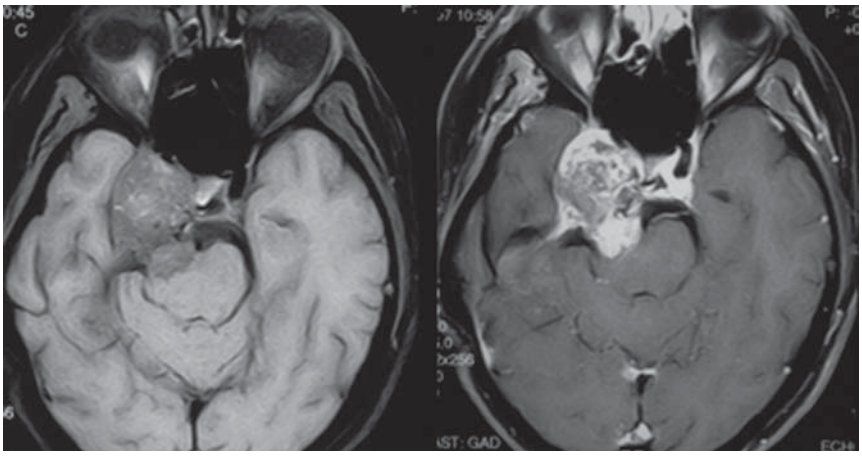

**Figure 16.** Right parasellar neurinoma of the trigeminal nerve (axial T1-weighted imaging before and after contrast administration).

### Dermoid and Epidermoid Tumors

Both dermoid and epidermoid tumors are benign, slow-growing congenital lesions which result from inclusion of epithelial elements during embryogenesis. They may cause mass effect in the sellar, parasellar or suprasellar region resulting in visual disturbance or endocrine dysfunction and account for < 2% of all intracranial neoplasms. Epidermoids are often hypointense in T1- and hyperintense in T2-weighted images (Figure 13). Depending upon their fat or calcium content, dermoid tumors can also show a hyper- or hypointense signal in T1 [95, 96] (Figure 14). For epidermoid tumors, diffusion-weighted images are helpful, as they typically show a markedly increased signal.

### Hypothalamic Hamartomas

Hypothalamic hamartomas are of neuronal origin and represent congenital heterotopias usually located within the tuber cinereum. They usually affect children, who present with precocious puberty and epileptic, typically gelastic seizures [97]. Characteristically, MRI and CT show a rounded expansion of the tuber cinereum, best seen in coronal and sagittal images. Hamartomas are isointense to the cerebral cortex in both T1- and T2-weighted images (Figure 15). Since they are rarely larger than 1–2 cm in diameter, little mass effect is seen [98, 99].

### Schwannomas/Neurinomas

Nerve sheath tumors in the parasellar region are very rare lesions and usually arise from the trigeminal nerve (V1/V2) or the third, fourth and sixth cranial nerve [100]. They are slow-growing tumors, and rarely, bony remodeling of the lateral portion of the sella or the apex of the petrous bone can be seen. Expansions through the superior orbital fissure or

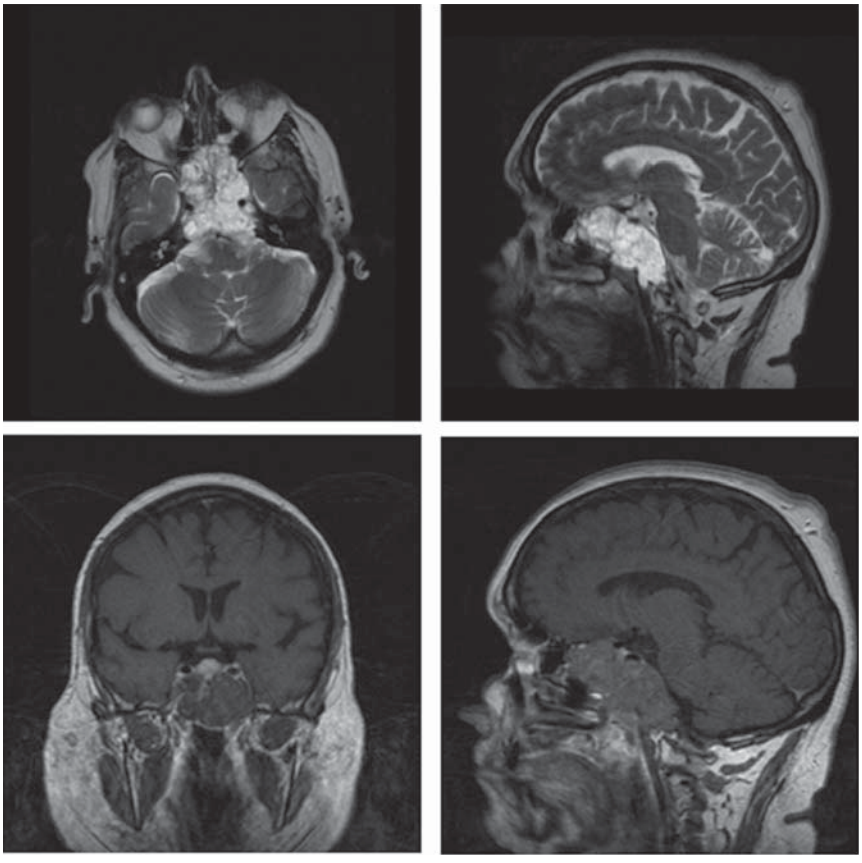

**Figure 17.** Extensive clival chordoma with its typical heterogeneous configuration (axial and sagittal T2-weighted imaging, contrast-enhanced coronal and sagittal T1-weighted imaging).

the oval and round foramen are published. On MRI and CT, they show an intense (usually heterogeneous) contrast enhancement (Figure 16) [101, 102].

### Tolosa-Hunt Syndrome

The Tolosa-Hunt syndrome is a painful, recurrent ophthalmoplegia that usually responds favorably to steroid medication. It is associated with granulomatous inflammatory changes at the cavernous sinus and the superior orbital fissure and can frequently affect various cranial nerves located within this area [103]. Contrast-enhanced MRI and CT show an asymmetric expansion of the cavernous sinus up to the superior orbital fissure or the orbital region [104–106].

### Cavernous Sinus Thrombosis

Thrombosis of the cavernous sinus is a rare condition and often secondary to iatrogenic or septic etiologies [107, 108]. On MRI and CT, enlargement of the cavernous sinus with internal filling defects and incomplete enhancement of the sinus may be noted. MR images might show high-signal thrombus within the cavernous sinus [109]. Additionally, periorbital edema, exophthalmus or dilatation of the superior ophthalmic vein can occur.

### Neoplasms Involving the Clivus

Neoplasms in the clival region can include chordoma, chondrosarcoma, hemangiopericytoma [110], meningioma, lymphoma [111], plasmocytoma, paraganglioma [112], or metastasis. With an incidence < 1%, chordoma and chondrosarcoma are even rarer than malformative tumors [113]. Clival chordoma is a slow-growing tumor arising from the remnants of the primitive notochord. It shows no age or sex predilection, usually causes bony destruction and can reach considerable size at the time of diagnosis. This extracranial tumor is heterogeneously hyperintense on T2-weighted images and shows a marked contrast enhancement (Figure 17). Chondroma is another bone-destructive, nodular/lobular tumor that tends to undergo mucinous, cystic regression and calcification. It most commonly arises from cartilaginous remnants in the area of the foramen lacerum. Imaging findings are similar to those in chordoma. Clival tumors tend to extend posteriorly into the prepontine cistern [114–117].

### Neoplasms Involving the Sphenoid Sinus

Mucoceles are the most common space-occupying mass lesions of the sphenoid sinus. The pathogenesis relates to obstruction of the sphenoid ostium (secondary mucocele) or mucous retention cyst expansion (primary mucocele). On CT, a nondestructive mass, causing a thinning and bulging of the bony sinus walls may be seen. The sellar contents can mimic a para- or suprasellar mass. MRI better demonstrates the wall-enhancing fluid-filled lesion [118–120]. Rarely, inverted papillomas arising from the ethmoid cells can extend to the sphenoid sinus.

## Conflict of Interest Statement

We certify that there is no actual or potential conflict of interest in relation to this article.

## References


1. Cox TD, Elster AD. Normal pituitary gland: changes in shape, size, and signal intensity during the 1st year of life at MR imaging. Radiology 1991;179:721–4.
2. Dietrich RB, Lis LE, Greensite FS, et al. Normal MR appearance of the pituitary gland in the first 2 years of life. AJNR Am J Neuroradiol 1995; 16:1413–9.
3. Elster AD. Modern imaging of the pituitary. Radiology 1993;187:1–14.
4. Fujisawa I, Nishimura K, Asato R, et al. Posterior lobe of the pituitary in diabetes insipidus: MR findings. J Comput Assist Tomogr 1987; 11:221–5.
5. Naylor MF, Scheithauer BW, Forbes GS, et al. Rathke cleft cyst: CT, MR, and pathology of 23 cases. J Comput Assist Tomogr 1995;19:853–9.
6. Brassier G, Morandi X, Tayiar E, et al. Rathke's cleft cysts: surgical-MRI correlation in 16 symptomatic cases. J Neuroradiol 1999;26:162–71.
7. Harter LP, Silverberg GD, Brant-Zawadzki M. Intrasellar arachnoid cyst: case report. Neurosurgery 1980;7:387–90.
8. Nomura M, Tachibana O, Hasegawa M, et al. Contrast-enhanced MRI of intrasellar arachnoid cysts: relationship between the pituitary gland and cyst. Neuroradiology 1996;38:566–8.
9. Starzyk J, Kwiatkowski S, Urbanowicz W, et al. Suprasellar arachnoidal cyst as a cause of precocious puberty – report of three patients and literature overview. J Pediatr Endocrinol Metab 2003;16:447–55.
10. Radhakrishnan K, Thacker AK, Bohlaga NH, et al. Epidemiology of idiopathic intracranial hypertension: a prospective and case-control study. J Neurol Sci 1993;116:18–28.
11. Skau M, Brennum J, Gjerris F, et al. What is new about idiopathic intracranial hypertension? An updated review of mechanism and treatment. Cephalalgia 2006;26:384–99.
12. Bergland RM, Ray BS, Torack RM. Anatomical variations in the pituitary gland and adjacent structures in 225 human autopsy cases. J Neurosurg 1968;28:93–9.
13. Argyropoulou M, Perignon F, Brunelle F, et al. Height of normal pituitary gland as a function of age evaluated by magnetic resonance imaging in children. Pediatr Radiol 1991;21:247–9.
14. Tsunoda A, Okuda O, Sato K. MR height of the pituitary gland as a function of age and sex: especially physiological hypertrophy in adolescence and in climacterium. AJNR Am J Neuroradiol 1997;18:551–4.
15. Abrahams JJ, Trefelner E, Boulware SD. Idiopathic growth hormone deficiency: MR findings in 35 patients. AJNR Am J Neuroradiol 1991;12:155–60.
16. Argyropoulou M, Perignon F, Brauner R, et al. Magnetic resonance imaging in the diagnosis of growth hormone deficiency. J Pediatr 1992;120:886–91.
17. Hamilton J, Blaser S, Daneman D. MR imaging in idiopathic growth hormone deficiency. AJNR Am J Neuroradiol 1998;19:1609–15.

18. Kornreich L, Horev G, Lazar L, et al. MR findings in growth hormone deficiency: correlation with severity of hypopituitarism. AJNR Am J Neuroradiol 1998;19:1495–9.
19. Fujisawa I, Kikuchi K, Nishimura K, et al. Transection of the pituitary stalk: development of an ectopic posterior lobe assessed with MR imaging. Radiology 1987;165:487–9.
20. Kelly WM, Kucharczyk W, Kucharczyk J, et al. Posterior pituitary ectopia: an MR feature of pituitary dwarfism. AJNR Am J Neuroradiol 1988; 9:453–60.
21. Saeki N, Tokunaga H, Wagai N, et al. MRI of ectopic posterior pituitary bright spot with large adenomas: appearances and relationship to transient postoperative diabetes insipidus. Neuroradiology 2003; 45:713–6.
22. Colao A, Lombardi G. Growth-hormone and prolactin excess. Lancet 1998;352:1455–61.
23. Calle-Rodrigue RD, Giannini C, Scheithauer BW, et al. Prolactinomas in male and female patients: a comparative clinicopathologic study. Mayo Clin Proc 1998;73:1046–52.
24. Carter JN, Tyson JE, Tolis G, et al. Prolactin-screening tumors and hypogonadism in 22 men. N Engl J Med 1978;299:847–52.
25. Melmed S. Acromegaly. N Engl J Med 1990;322:966–77.
26. Holdaway IM, Rajasoorya CR, Gamble GD, et al. Long-term treatment outcome in acromegaly. Growth Horm IGF Res 2003;13:185–92.
27. Orme SM, McNally RJ, Cartwright RA, et al. Mortality and cancer incidence in acromegaly: a retrospective cohort study. United Kingdom Acromegaly Study Group. J Clin Endocrinol Metab 1998; 83:2730–4.
28. Magiakou MA, Mastorakos G, Oldfield EH, et al. Cushing's syndrome in children and adolescents. Presentation, diagnosis, and therapy. N Engl J Med 1994;331:629–36.
29. Sonino N, Boscaro M. Medical therapy for Cushing's disease. Endocrinol Metab Clin North Am 1999;28:211–22.
30. Nelson DH. Cushing's syndrome – pituitary or adrenal origin? J Chronic Dis 1960;12:499–503.
31. Nelson DH, Meakin JW, Thorn GW. ACTH-producing pituitary tumors following adrenalectomy for Cushing's syndrome. Ann Intern Med 1960;52:560–9.
32. Beck Peccoz P, Brucker-Davis F, Persani L, et al. Thyrotropin-secreting pituitary tumors. Endocr Rev 1996;17:610–38.
33. Ebersold MJ, Quast LM, Laws ER Jr, et al. Long-term results in transsphenoidal removal of nonfunctioning pituitary adenomas. J Neurosurg 1986;64:713–9.
34. Snyder PJ. Clinically nonfunctioning pituitary adenomas. Endocrinol Metab Clin North Am 1993;22:163–75.
35. Aaberg TM Jr, Kay M, Sternau L. Metastatic tumors to the pituitary. Am J Ophthalmol 1995;119:779–85.
36. Mayr NA, Yuh WT, Muhonen MG, et al. Pituitary metastases: MR findings. J Comput Assist Tomogr 1993;17:432–7.
37. Donovan JL, Nesbit GM. Distinction of masses involving the sella and suprasellar space: specificity of imaging features. AJR Am J Roentgenol 1996;167:597–603.
38. Kovacs K. Adenohypophysial necrosis in routine autopsies. Endokrinologie 1972;60:309–16.
39. Rolih CA, Ober KP. Pituitary apoplexy. Endocrinol Metab Clin North Am 1993;22:291–302.
40. Vidal E, Cevallos R, Vidal J, et al. Twelve cases of pituitary apoplexy. Arch Intern Med 1992;152:1893–9.
41. Bonicki W, Kasperlik-Zaluska A, Koszewski W, et al. Pituitary apoplexy: endocrine, surgical and oncological emergency. Incidence, clinical course and treatment with reference to 799 cases of pituitary adenomas. Acta Neurochir (Wien) 1993;120:118–22.
42. Randeva HS, Schoebel J, Byrne J, et al. Classical pituitary apoplexy: clinical features, management and outcome. Clin Endocrinol (Oxf) 1999;51:181–8.
43. Kulkarni MV, Lee KF, McArdle CB, et al. 1.5-T MR imaging of pituitary microadenomas: technical considerations and CT correlation. AJNR Am J Neuroradiol 1988;9:5–11.
44. Bartynski WS, Lin L. Dynamic and conventional spin-echo MR of pituitary microlesions. AJNR Am J Neuroradiol 1997;18:965–72.
45. Rand T, Lippitz P, Kink E, et al. Evaluation of pituitary microadenomas with dynamic MR imaging. Eur J Radiol 2002;41:131–5.
46. Stadnik T, Spruyt D, van Binst A, et al. Pituitary microadenomas: diagnosis with dynamic serial CT, conventional CT and T1-weighted MR imaging before and after injection of gadolinium. Eur J Radiol 1994; 18:191–8.
47. Tabarin A, Laurent F, Catargi B, et al. Comparative evaluation of conventional and dynamic magnetic resonance imaging of the pituitary gland for the diagnosis of Cushing's disease. Clin Endocrinol (Oxf) 1998;49:293–300.
48. Yuh WT, Fisher DJ, Nguyen HD, et al. Sequential MR enhancement pattern in normal pituitary gland and in pituitary adenoma. AJNR Am J Neuroradiol 1994;15:101–8.
49. Teng MM, Huang CI, Chang T. The pituitary mass after transsphenoidal hypophysectomy. AJNR Am J Neuroradiol 1988;9:23–6.
50. Kilic T, Ekinci G, Seker A, et al. Determining optimal MRI follow-up after transsphenoidal surgery for pituitary adenoma: scan at 24 hours postsurgery provides reliable information. Acta Neurochir (Wien) 2001; 143:1103–26.
51. Abrams HL, Spiro R, Goldstein N. Metastases in carcinoma; analysis of 1000 autopsied cases. Cancer 1950;3:74–85.
52. Pernicone PJ, Scheithauer BW, Sebo TJ, et al. Pituitary carcinoma: a clinicopathologic study of 15 cases. Cancer 1997;79:804–12.
53. Scheithauer BW, Kurtkaya-Yapicier O, Kovacs KT, et al. Pituitary carcinoma: a clinicopathological review. Neurosurgery 2005;56: 1066–74.
54. Fujii K, Fujita N, Hirabuki N, et al. Neuromas and meningiomas: evaluation of early enhancement with dynamic MR imaging. AJNR Am J Neuroradiol 1992;13:1215–20.
55. Joo YG, Korogi Y, Hirai T, et al. Differential diagnosis of extra-axial intracranial tumours by dynamic spin-echo MRI. Neuroradiology 1995; 37:522–5.
56. Cappabianca P, Cirillo S, Alfieri A, et al. Pituitary macroadenoma and diaphragm sellae meningioma: differential diagnosis on MRI. Neuroradiology 1999;41:22–6.
57. Pinzer T, Krishnan KG, Schackert G. The diaphragma sellae meningioma – a rare differential diagnosis of non-functioning pituitary adenoma. Zentralbl Neurochir 2004;65:195–7.
58. Michael AS, Paige ML. MR imaging of intrasellar meningiomas simulating pituitary adenomas. J Comput Assist Tomogr 1988;12:944–6.
59. Nozaki K, Nagata I, Yoshida K, et al. Intrasellar meningioma: case report and review of the literature. Surg Neurol 1997;47:447–52.
60. Yeakley JW, Kulkarni MV, McArdle CB, et al. High-resolution MR imaging of juxtasellar meningiomas with CT and angiographic correlation. AJNR Am J Neuroradiol 1988;9:279–85.
61. Hoffman HJ. Surgical management of craniopharyngioma. Pediatr Neurosurg 1994;21:Suppl 1:44–9.
62. Sartoretti-Schefer S, Wichmann W, Aguzzi A, et al. MR differentiation of adamantinous and squamous-papillary craniopharyngiomas. AJNR Am J Neuroradiol 1997;18:77–87.
63. Nagahata M, Hosoya T, Kayama T, et al. Edema along the optic tract: a useful MR finding for the diagnosis of craniopharyngiomas. AJNR Am J Neuroradiol 1998;19:1753–7.
64. Saeki N, Uchino Y, Murai H, et al. MR imaging study of edema-like change along the optic tract in patients with pituitary region tumors. AJNR Am J Neuroradiol 2003;24:336–42.
65. Eldevik OP, Blaivas M, Gabrielsen TO, et al. Craniopharyngioma: radiologic and histologic findings and recurrence. AJNR Am J Neuroradiol 1996;17:1427–39.

66. Cho DY, Wang YC, Ho WL. Primary intrasellar mixed germ-cell tumor with precocious puberty and diabetes insipidus. Childs Nerv Syst 1997;13:42–6.
67. Jennings MT, Gelman R, Hochberg F. Intracranial germ-cell tumors: natural history and pathogenesis. J Neurosurg 1985;63:155–67.
68. Bubl R, Hugo HH, Hempelmann RG, et al. Granular-cell tumour: a rare suprasellar mass. Neuroradiology 2001;43:309–12.
69. Wilkinson MD, Fulham MJ, Besser M. Neuroimaging findings in a suprasellar granular cell tumor. J Comput Assist Tomogr 2003;27:26–9.
70. Isidro ML, Iglesias Diaz P, Matias Guiu X, et al. Acromegaly due to a growth hormone-releasing hormone-secreting intracranial gangliocytoma. J Endocrinol Invest 2005;28:162–5.
71. Song JK, Weil RJ. Pathologic quiz case: an unusual cause of acromegaly. Intrasellar gangliocytoma. Arch Pathol Lab Med 2005; 129:415–6.
72. Lopes MB, Lanzino G, Cloft HJ, et al. Primary fibrosarcoma of the sella unrelated to previous radiation therapy. Mod Pathol 1998; 11:579–84.
73. Moro M, Giannini C, Scheithauer BW, et al. Combined sellar fibrosarcoma and prolactinoma with neuronal metaplasia: report of a case unassociated with radiotherapy. Endocr Pathol 2004;15:149–58.
74. Gharbi A, Ousehal A, Kissani N, et al. [Sellar hemangiopericytoma. Report of a case.] J Neuroradiol 2001;28:195–9.
75. Sarwar M. Primary sellar-parasellar esthesioneuroblastoma. AJR Am J Roentgenol 1979;133:140–1.
76. Jacob S, Pye E, Hbahbih M, et al. Rapidly progressive bilateral ophthalmoplegia and enlarging sellar mass caused by amelanotic melanoma. J Neuroophthalmol 2006;26:49–50.
77. Kimura M, Takayasu M, Suzuki Y, et al. Primary choroid plexus papilloma located in the suprasellar region: case report. Neurosurgery 1992; 31:563–6.
78. Huang YY, Lin SF, Dunn P, et al. Primary pituitary lymphoma presenting as hypophysitis. Endocr J 2005;52:543–9.
79. Atlas SW, Grossman RI, Goldberg HI, et al. Partially thrombosed giant intracranial aneurysms: correlation of MR and pathologic findings. Radiology 1987;162:111–4.
80. Guoth MS, Kim J, de Lotbiniere AC, et al. Neurosarcoidosis presenting as hypopituitarism and a cystic pituitary mass. Am J Med Sci 1998; 315:220–4.
81. Bellastella A, Bizzarro A, Coronella C, et al. Lymphocytic hypophysitis: a rare or underestimated disease? Eur J Endocrinol 2003; 149:363–76.
82. Leung GK, Lopes MB, Thorner MO, et al. Primary hypophysitis: a single-center experience in 16 cases. J Neurosurg 2004;101:262–71.
83. Thodou E, Asa SL, Kontogeorgos G, et al. Clinical case seminar: lymphocytic hypophysitis: clinicopathological findings. J Clin Endocrinol Metab 1995;80:2302–11.
84. Saiwai S, Inoue Y, Ishihara T, et al. Lymphocytic adenohypophysitis: skull radiographs and MRI. Neuroradiology 1998;40:114–20.
85. Basaria S, Ayala AR, Guerin C, et al. A rare pituitary lesion. J Endocrinol Invest 2000;23:189–92.
86. Bullmann C, Faust M, Hoffmann A, et al. Five cases with central diabetes insipidus and hypogonadism as first presentation of neurosarcoidosis. Eur J Endocrinol 2000;142:365–72.
87. Goyal M, Kucharczyk W, Keystone E. Granulomatous hypophysitis due to Wegener's granulomatosis. AJNR Am J Neuroradiol 2000; 21:1466–9.
88. Honegger J, Fahlbusch R, Bornemann A, et al. Lymphocytic and granulomatous hypophysitis: experience with nine cases. Neurosurgery 1997;40:713–22.
89. Sato N, Sze G, Endo K. Hypophysitis: endocrinologic and dynamic MR findings. AJNR Am J Neuroradiol 1998;19:439–44.
90. Jadhav RN, Dahiwadkar HV, Palande DA. Abscess formation in invasive pituitary adenoma: case report. Neurosurgery 1998;43:616–9.
91. Milligan SA, Katz MS, Craven PC, et al. Toxoplasmosis presenting as panhypopituitarism in a patient with the acquired immune deficiency syndrome. Am J Med 1984;77:760–4.
92. Maartens NF, Ellegala DB, Lopes MB. Pituitary abscess. J Neurosurg 2001;95:1110–2.
93. Sabbah P, Bonardel G, Herve R, et al. CT and MRI findings in primitive pituitary abscess: a case report and review of literature. J Neuroradiol 1999;26:196–9.
94. Vates GE, Berger MS, Wilson CB. Diagnosis and management of pituitary abscess: a review of twenty-four cases. J Neurosurg 2001; 95:233–41.
95. Civit T, Marchal JC, Pinelli C, et al. Intrasellar epidermoid cysts. Neurochirurgie 1999;45:150–4.
96. Yasargil MG, Abernathey CD, Sarioglu AC. Microneurosurgical treatment of intracranial dermoid and epidermoid tumors. Neurosurgery 1989;24:561–7.
97. Judge DM, Kulin HE, Page R, et al. Hypothalamic hamartoma: a source of luteinizing-hormone-releasing factor in precocious puberty. N Engl J Med 1977;296:7–10.
98. Amstutz DR, Coons SW, Kerrigan JF, et al. Hypothalamic hamartomas: Correlation of MR imaging and spectroscopic findings with tumor glial content. AJNR Am J Neuroradiol 2006;27:794–8.
99. Freeman JL, Coleman LT, Wellard RM, et al. MR imaging and spectroscopic study of epileptogenic hypothalamic hamartomas: analysis of 72 cases. AJNR Am J Neuroradiol 2004;25:450–62.
100. Wilberger JE Jr. Primary intrasellar schwannoma: case report. Surg Neurol 1989;32:156–8.
101. Johnsen DE, Woodruff WW, Allen IS, et al. MR imaging of the sellar and juxtasellar regions. Radiographics 1991;11:727–58.
102. Whee SM, Lee JI, Kim JH. Intrasellar schwannoma mimicking pituitary adenoma: a case report. J Korean Med Sci 2002;17:147–50.
103. Kline LB, Hoyt WF. The Tolosa-Hunt syndrome. J Neurol Neurosurg Psychiatry 2001;71:577–82.
104. De Arcaya AA, Cerezal L, Canga A, et al. Neuroimaging diagnosis of Tolosa-Hunt syndrome: MRI contribution. Headache 1999; 39:321–5.
105. Haque TL, Miki Y, Kashii S, et al. Dynamic MR imaging in Tolosa–Hunt syndrome. Eur J Radiol 2004;51:209–17.
106. Odabasi Z, Gokcil Z, Atilla S, et al. The value of MRI in a case of Tolosa-Hunt syndrome. Clin Neurol Neurosurg 1997;99:151–4.
107. DiNubile MJ. Septic thrombosis of the cavernous sinuses. Arch Neurol 1988;45:567–72.
108. Ebright JR, Pace MT, Niazi AF. Septic thrombosis of the cavernous sinuses. Arch Intern Med 2001;161:2671–6.
109. Schuknecht B, Simmen D, Yuksel C, et al. Tributary venosinus occlusion and septic cavernous sinus thrombosis: CT and MR findings. AJNR Am J Neuroradiol 1998;19:617–26.
110. Morrison DA, Bibby K. Sellar and suprasellar hemangiopericytoma mimicking pituitary adenoma. Arch Ophthalmol 1997;115:1201–3.
111. Landman RE, Wardlaw SL, McConnell RJ, et al. Pituitary lymphoma presenting as fever of unknown origin. J Clin Endocrinol Metab 2001; 86:1470–6.
112. Naggara O, Varlet P, Page P, et al. Suprasellar paraganglioma: a case report and review of the literature. Neuroradiology 2005;47:753–7.
113. Freda PU, Post KD. Differential diagnosis of sellar masses. Endocrinol Metab Clin North Am 1999;28:81–117.
114. Allan CA, Kaltsas G, Evanson J, et al. Pituitary chondrosarcoma: an unusual cause of a sellar mass presenting as a pituitary adenoma. J Clin Endocrinol Metab 2001;86:386–91.
115. Gay E, Sekhar LN, Rubinstein E, et al. Chordomas and chondrosarcomas of the cranial base: results and follow-up of 60 patients. Neurosurgery 1995;36: 887–96.
116. Lee HJ, Kalnin AJ, Holodny AI, et al. Hemorrhagic chondroid chordoma mimicking pituitary apoplexy. Neuroradiology 1998;40:720–3.

117. Rosenberg AE, Nielsen GP, Keel SB, et al. Chondrosarcoma of the base of the skull: a clinicopathologic study of 200 cases with emphasis on its distinction from chordoma. Am J Surg Pathol 1999; 23:1370–8.
118. Akan H, Cihan B, Celenk C. Sphenoid sinus mucocele causing third nerve paralysis: CT and MR findings. Dentomaxillofac Radiol 2004; 33:342–4.
119. Di Girolamo S, Cannizzaro P, Picciotti P, et al. Ophthalmoplegia and ptosis as onset symptoms of an isolated primary mucocele of the sphenoid sinus. J Oral Maxillofac Surg 2002;60:1500–2.
120. Som PM. CT of the paranasal sinuses. Neuroradiology 1985;27: 189–201.

**Address for Correspondence**
Arnd Doerfler, MD, PhD, MA
Department of Neuroradiology
University of Erlangen-Nuremberg
Schwabachanlage 6
91054 Erlangen
Germany
Phone (+49/9131) 85-34326, Fax -3679
e-mail: arnd.doerfler@uk-erlangen.de